

# Studies on Neutron, Photon (Bremsstrahlung) and Proton Induced Fission of Actinides and Pre-Actinides

H. NAIK<sup>1</sup>, G.N. KIM<sup>2</sup>, S.V. SURYANARAYANA<sup>3</sup>, K.S. KIM<sup>2</sup>, M.W. LEE<sup>2</sup>,  
GANESH SANJEEV<sup>4</sup>, V.T. NIMJE<sup>5</sup>, K.C. MITTAL<sup>5</sup> S. GANESAN<sup>6</sup> AND  
A.GOSWAMI<sup>1</sup>

<sup>1</sup>Radiochemistry Division, BARC, Mumbai- 400 085, India

<sup>2</sup>Department of Physics, Kyungpook National University, Daegu702-701, Republic of Korea

<sup>3</sup>Nuclear Physics Division, BARC, Mumbai- 400 085, India

<sup>4</sup>Microtron Centre, Department of Studies in Physics, Mangalore University, Mangalagangothri-574 199, Karnataka, India.

<sup>5</sup>Accelerator and Pulse Power Division, BARC, Mumbai- 400 085, India

<sup>6</sup>Reactor Physics Design Division, BARC, Mumbai- 400 085, India

\*Email:naikhbarc@gmail.com

Received: April 06, 2015 | Revised: April 20, 2015 | Accepted: May 11, 2015

Published online: August 03, 2015

The Author(s) 2015. This article is published with open access at [www.chitkara.edu.in/publications](http://www.chitkara.edu.in/publications)

**Abstract:** We present the yields of various fission products determined in the reactor neutron, 3.7-18.1 MeV quasi-mono energetic neutron, 8-80 MeV bremsstrahlung and 20-45 MeV proton induced fission of <sup>232</sup>Th and <sup>238</sup>U using radiochemical and off-line beta or gamma ray counting. The yields of the fission products in the bremsstrahlung induced fission <sup>nat</sup>Pb and <sup>209</sup>Bi with 50-70 MeV and 2.5 GeV based on off-line gamma ray spectrometric technique were also presented. From the yields of fission products, the mass chains yields were obtained using charge distribution correction. From the mass yield distribution, the peak-to-valley (P/V) ratio was obtained. The role of excitation energy on the peak-to-valley ratio and fine structure such as effect of shell closure proximity and even-odd effect of mass yield distribution were examined. The higher yields of the fission products around A=133-134, 138-140 and 143-144 and their complementary products explained from the nuclear structure effect and role of standard I and II mode of asymmetric fission. In the neutron, photon (bremsstrahlung) and proton induced fission, the asymmetric mass distribution for actinides (Th, U) and symmetric

Journal of Nuclear  
Physics, Material  
Sciences, Radiation  
and Applications  
Vol. 3, No. 1  
August 2015  
pp. 55-73

Naik, H  
 Kim, GN  
 Suryanarayana, SV  
 Kim, KS  
 Lee, MW  
 Sanjeev, G  
 Nimje, VT  
 Mittal, KC  
 Ganesan, S  
 Goswami, A

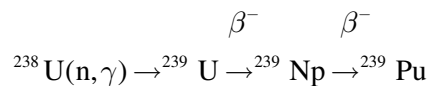
---

distribution for pre-actinides (Pb, Bi) were explained from different type of potential fission barrier.

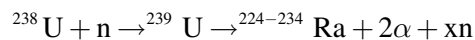
**Keywords:** Fission products yields, mass yield distribution, photon, neutron and proton induced fission, actinides ( $^{232}\text{Th}$ ,  $^{238}\text{U}$ ), pre-actinides ( $^{\text{nat}}\text{Pb}$ ,  $^{209}\text{Bi}$ ), nuclear structure effect.

## 1. INTRODUCTION

Discovery of neutron by Chadwick [25] and radioactivity by Curie and Joliot [2] prompted Fermi and coworkers [6, 7] in 1934 to attempt similar study of nuclear transmutation by neutron bombardment. Using uranium as the target, they were able to separate several radioactive products that were believed to be trans-uranium elements. At that time, it was assumed that the production of trans-uranium element based on the following reaction



Following Fermi [7], Hahn and Strassmann [32] as well as Curie and Savitch [21] in 1937 took special interest for the separation of the radio-activities, produced in the bombardment of neutrons on uranium. Using barium as carrier, they [32] were able to separate some of the radio-activities that were believed to be the isotopes of radium produced from  $^{238}\text{U}(\text{n}, 2\alpha, \text{xn})\text{Ra}$  reaction. i.e



However, fractional crystallization carried out by them indicated that the activities were really due to the isotopes of barium. i.e.



From the above observation they realized that with the absorption of neutron, heavy nuclei (Uranium) divides into two smaller nuclei of comparable masses like barium and krypton. This finding forced them to conclude about the discovery of a new type of nuclear reaction. Meitner and Frisch [19] give the name as nuclear fission analogous to the process of biological cell division.

Hahn and Strassmann [32] further observed that the division is not always the same in terms of A and Z of the resultant products and it takes place in many ways due to which a large number of radioactive nuclides are produced. It was also realized that enormous amount of energy equivalent to the net change of binding energy is released in the fission process. i.e.

---

$$[(\Delta_U + \Delta_n) - (\Delta_{Ba} + \Delta_{Kr})] \times 931 \text{ MeV} \geq 200 \text{ MeV}$$

Frisch [33] was the first to demonstrate this large amount of energy release in the form of large pulse height produced in ionization chamber experiment. Quantitative estimate of the energy release of about 200 MeV was calculated first by Bohr [31] considering fissioning nucleus as liquid drop. As explained by him, the fission of uranium nucleus by thermal neutron was due to the 0.7%  $^{235}\text{U}$  isotope. The mechanism of nuclear fission was explained by Bohr and Wheeler [30] based on liquid drop model. However, so many unexplained phenomenon of liquid drop model was explained by the development of double humped fission barrier of Strutinsky et al. [42].

Since the discovery of nuclear fission, large amount of experimental and theoretical work has been carried out with a view to understand the mechanism of nuclear fission. Experimental work carried out using either physical or radiochemical techniques were aimed to explain the fission cross-sections, their dependence on excitation energy, mass and charge yield distributions, kinetic energy distributions, prompt neutron and gamma ray multiplicities, fragment angular distribution and fragment angular momentum etc. The experimental work carried out so far can be obtained from two main text books [38, 4] whereas, the fission product yield data were available from EXFOR [23] compilation and various evaluations [3, 27, 29]. Similarly, various theoretical models [2, 34, 37] were also available and proposed in course of time to explain the new observations, which in turn enhanced the understanding of nuclear fission in comprehensive way.

In this manuscript, determination of the yields of various fission products and the mass yield distribution in the fast neutron induced fission of  $^{232}\text{Th}$  and  $^{238}\text{U}$ , which were determined experimentally at BARC using reactor APSARA and  $^7\text{Li}(p,n)$  neutron from BARC-TIFR pelletron facility and their outcome relevance to fission mechanism is discussed [11, 39-40]. The mass yield distribution in the bremsstrahlung induced fission of pre-actinides ( $^{\text{nat}}\text{Pb}$ ,  $^{209}\text{Bi}$ ) with the 50-70 MeV and 2.5 GeV and actinides ( $^{232}\text{Th}$ ,  $^{238}\text{U}$ ) with 8-80 MeV as well as proton induced fission of  $^{232}\text{Th}$  with 20-45 MeV, which were carried out by us [8-10, 12-19, 35] in India and South Korea is described.

## 2. EXPERIMENTAL PROCEDURE

In the case of reactor neutron irradiation, the experiment was carried out by using the light-water moderated highly enriched uranium fuelled swimming pool reactor APSARA at BARC, India [11, 40]. About 10 gram of oxide of  $^{232}\text{Th}$  and 5 mg of oxide of  $^{238}\text{U}$  (99.9997 % pure) were wrapped into a 0.025

---

Naik, H  
Kim, GN  
Suryanarayana, SV  
Kim, KS  
Lee, MW  
Sanjeev, G  
Nimje, VT  
Mittal, KC  
Ganesan, S  
Goswami, A

---

mm thick aluminum foil of appropriate size. For the reactor neutron induced fission of  $^{232}\text{Th}$ , about 0.5 gram of  $^{\text{nat}}\text{U}$  was also wrapped with 0.025 mm thick Al foil separately [39]. Both the targets were wrapped with another piece of super pure aluminum foil. For the reactor neutron induced fission of  $^{238}\text{U}$ , about 20  $\mu\text{l}$  of dilute nitric acid solution of  $^{238}\text{U}$  of concentration 1.42 mg/ml was taken in a polypropylene tube of approximately 4 cm length and 3 mm ID and open at one end [11, 40]. Two small strips of lexan track detector were then put into the solution and the polypropylene tube was heat sealed. The uranium target and the sealed polypropylene tube were wrapped in 1 mm thick cadmium foil to reduce the formation of  $^{239}\text{U}$  and its daughter  $^{239}\text{Np}$  during the neutron irradiation as their gamma rays otherwise interfere with the gamma ray spectrum of the fission products. The Al wrapped target of  $^{232}\text{Th}+^{\text{nat}}\text{U}$  and the Al+Cd wrapped solution oxide of  $^{238}\text{U}+$  nitrate solution of  $^{238}\text{U}$  were triple sealed in alkathene bags. The target assembly was then irradiated for 15 min to 40 h in a fixed position of the reactor APSARA at a flux of  $10^{11} \text{ n cm}^{-2} \text{ s}^{-1}$ . The fission products from the irradiated  $^{232}\text{Th}$  target after radiochemical separation were analyzed by beta and gamma ray counting using beta proportional and NaI(Tl) scintillator counter, respectively. On the other hand, the fission products from the irradiated  $^{238}\text{U}$  target with or without radiochemical separation were analyzed by off-line gamma ray spectrometric technique using HPGe detector coupled to a PC based 4-K channel analyzer. The resolution of the detector system was 2.0 keV full width at half maximum (FWHM) at the 1332.0 keV  $\gamma$ -line of  $^{60}\text{Co}$ .

In the case of high energy of 3.7-18.2 MeV quasi-mono-energetic neutron irradiation, the experiment was carried out using the 14 UD BARC-TIFR Pelletron facility at TIFR, Mumbai, India [18, 35]. The neutron beam was obtained from the  $^7\text{Li}(p, n)$  reaction by using the proton beam main line at 6 m above the analyzing magnet of the Pelletron facility to utilize the maximum proton current from the accelerator. The lithium foil was made up of natural lithium with thickness of  $3.7 \text{ mg/cm}^2$ , sandwiched between two tantalum foils of different thickness. The front tantalum foil facing the proton beam is the thinnest one, with thickness of  $3.9 \text{ mg/cm}^2$ , in which the proton degradation of the proton energy is only 30 keV. On the other hand, the back tantalum foil is of 0.025 mm thick, which is sufficient to stop the proton beam. Behind the Ta-Li-Ta stack, the samples used were 0.025 mm thick and  $1 \text{ cm}^2$  area natural  $^{232}\text{Th}$  and  $^{238}\text{U}$  metal foils wrapped in 0.025 mm thick aluminum foil. The Al wrapped sample of  $^{232}\text{Th}$  and  $^{238}\text{U}$  were mounted at a distance of 2.1 cm from the location of Li-Ta-Li stack at zero degree with respect to the beam direction. The Ta-Li-Ta stack and Al wrapped  $^{232}\text{Th}$  and  $^{238}\text{U}$  were irradiated for 4-12 hours depending upon the proton beam energy facing the tantalum

---

target. The proton current during the irradiation varies from 100 to 400 nA and beam energy from 5.6 to 20 MeV. The maximum quasi-neutron energies vary from 3.7 to 18.1 MeV corresponding to the proton energy of 5.6 to 20 MeV. After cooling time of 1-2 h, the fission products of the irradiated samples were analyzed by off-line gamma ray spectrometric technique using HPGe detector coupled to a PC based 4-K channel analyzer.

In the case of 20-45 MeV proton beam irradiations, the experiments were carried out by using two accelerators and at two different countries. The 19.55 MeV proton induced fission of  $^{232}\text{Th}$  was carried out by using 14UD BARC-TIFR Pelletron at Mumbai, India [10]. The proton beam at 6 m height above the analyzing magnet of the Pelletron was used to utilize the maximum proton current from the accelerator. For 32.21 and 44.76 MeV proton induced fission of  $^{232}\text{Th}$  was carried out using medical cyclotron (MC-50) at the Korea Institute of Radiological and Medical Science (KIRAMS) Seoul, Korea [10]. During the experiment, a collimator of 6 mm diameter for the 19.55 MeV proton irradiation and 10 mm diameter for 32.21 and 44.76 MeV proton irradiation before the target were used. The energy spread within the 20-45 MeV proton beam was only 50 to 90 keV. The natural  $^{232}\text{Th}$  metal target used for irradiation was of 0.025 mm thick and of 1 cm<sup>2</sup> size. The  $^{232}\text{Th}$  metal was covered with 0.025 mm thick super pure Al foil on both side of the target to make the Al-Th-Al stack. Th Al cover acts as catcher for the fission products recoiling out from the target during irradiation. In case of 14UD BARC-TIFR Pelletron, Al-Th-Al stack was wrapped with additional 0.025 mm thick Al. In case of medical cyclotron, in between two sets of Al-Th-Al stacks, a 3.8 mm thick Al was used as energy degrader. The two Al-Th-Al stack targets and thick Al degrader were also additionally wrapped with 0.025 mm thick Al. The stack of target was mounted at zero degree with respect to the beam direction. The first set of target was irradiated for 30 minutes with 20 MeV proton beam from the 14UD BARC-TIFR Pelletron at Mumbai. The second set of target stack was irradiated for 15 minutes with 45 MeV proton beam from the medical cyclotron (K-50) at (KIRAMS) Seoul. In the case of 14UD BARC-TIFR Pelletron, the proton current during irradiation was 300 nA and the proton energy faced by the Th target was 19.55 MeV after energy degradation on the two front Al of 0.025 mm thick each. In the medical cyclotron at Seoul, the proton current was 100 nA and the proton energies faced by the two Th targets were 32.21 and 44.76 MeV after the energy degradation based on the stack arrangement. After cooling time of 10 min to 0.5 h, the fission products from the Al catcher were analyzed by off-line gamma ray spectrometric technique using HPGe detector coupled to a PC based 4-K channel analyzer.

---

Naik, H  
Kim, GN  
Suryanarayana, SV  
Kim, KS  
Lee, MW  
Sanjeev, G  
Nimje, VT  
Mittal, KC  
Ganesan, S  
Goswami, A

---

In the case of bremsstrahlung irradiation of actinides ( $^{232}\text{Th}$ ,  $^{238}\text{U}$ ) and pre-actinides ( $^{\text{nat}}\text{Pb}$ ,  $^{209}\text{Bi}$ ), the experiments were carried out using the 8 MeV microtron at Mangalore [13] and 10 MeV electron linac at EBC centre, Kharghar, Navi-Mumbai, India [19] as well as the 100 MeV and 2.5 GeV electron linac at Pohang Accelerator Laboratory (PAL), Pohang, South Korea [8, 10, 12, 14-17]. In the 8 MeV microtron, the bremsstrahlung beam was produced by impinging pulsed electron beam on 0.188 cm thick tantalum target [13]. The Ta target, which acts as an electron to photon converter was located at a distance of 30 cm from the beam exit window. In the 10 MeV electron linac the bremsstrahlung beam was produced by impinging the pulsed electron beam on 1 mm thick tantalum metal foil placed at a distance of 10 cm on a suitable stand facing the electron beam aperture [19]. In the 100 MeV and 2.5 GeV electron linac the bremsstrahlung beam was produced by bombarding the 45-80 MeV and 2.5 GeV pulsed electron beam on a 0.1 and 1 mm thick W target located at a distance of 18-24 cm from the beam exit window [8, 10, 12, 14-17]. For actinides irradiation, 0.025 mm thick target  $^{232}\text{Th}$  and  $^{238}\text{U}$  with 0.25 to 1 cm<sup>2</sup> size were placed at a 3-38.5 cm distance from the electron to photon beam converter and irradiated for 15 min to 5 h [10, 13, 17, 19]. For pre-actinides irradiation, 0.5 mm thick and 25 cm<sup>2</sup> size  $^{\text{nat}}\text{Pb}$  and 3 mm thick and 25 cm<sup>2</sup> size  $^{209}\text{Bi}$  targets were placed at a 12-24 cm distance from the electron to photon beam converter and irradiated for 4-7 h [12-14]. During the irradiation, the 8 MeV microtron accelerator was operated with pulse repetition rate of 250 Hz, a pulse width of 2.42  $\mu\text{s}$  and beam current of 50 mA [13]. The 10 MeV electron linac was operated with pulse repetition rate of 300-400 Hz, a pulse width of 10  $\mu\text{s}$  and beam current of 100-200 mA [19]. The 100 MeV electron linac was with pulse repetition of 3.75 Hz, a beam width of 1.5  $\mu\text{s}$  and beam current of 15 mA [8, 10, 12, 15, 17]. The 2.5 GeV electron linac was with a pulse repetition rate of 10 Hz, a pulse width of 1 ns and beam current of 150 mA [16, 14]. After a cooling time of 0.25-2 h, the fission products of the irradiated samples were analyzed by off-line gamma ray spectrometric technique using HPGe detector coupled to a PC based 4-K channel analyzer.

### 3. CALCULATIONS (DATA ANALYSIS)

The yield of various fission products (X) in the reactor neutron induced fission of  $^{232}\text{Th}$  was obtained by Iyer et al. [39] in Radiochemistry division by using comparison method. In this method since U was always irradiated along with Th and same fission product was separated from both irradiated sample. The fission product  $^{99}\text{Mo}$  isolated from  $^{235}\text{U}(n, f)$  was used as internal standard.

Then the ratio (D) of any fission product activity ( $A_x$ ) with respect to Mo activity ( $A_{Mo}$ ) was obtained as

$$D_{Th} = (A_x)_{Th} / (A_{Mo})_{Th}, D_U = (A_x)_{U} / (A_{Mo})_{U} \quad (1)$$

$$R = D_{Th} / D_U, \text{ Activity } (A_x) = Y_x \lambda_x f \varepsilon_x \quad (2)$$

Studies on  
Neutron, Photon  
(Bremsstrahlung)  
and Proton  
Induced Fission of  
Actinides and  
Pre-Actinides

Where  $Y_x$  is the fission product yield of the particular nuclide,  $\lambda_x$  is the decay constant,  $f$  the total number of fission events taking place in the target and  $\varepsilon_x$  the counting efficiency of the beta or gamma ray of the fission products. Then

$$R = D_{Th} / D_U = \frac{(Y_x \lambda_x f \varepsilon_x)_{Th} / (Y_{Mo} \lambda_{Mo} f \varepsilon_{Mo})_{Th}}{(Y_x \lambda_x f \varepsilon_x)_{U} / (Y_{Mo} \lambda_{Mo} f \varepsilon_{Mo})_{U}} = \frac{(Y_x)_{Th} / (Y_{Mo})_{Th}}{(Y_x)_{U} / (Y_{Mo})_{U}} \quad (5)$$

$$Y_x = R Y'_{Mo} (Y_{Mo} / Y'_{Mo}) \quad (4)$$

If  $Y_{Mo} / Y'_{Mo}$  is arbitrary set equal to 1, then  $Y_x = R Y'_{Mo}$  is the relative yields of the fission product (X) in Th. Then the absolute yield is obtained by normalizing the area the relative mass yield curve to 200 %.

The absolute yield of various fission products in the epi-cadmium neutron induced fission of 99.9997 atom percent pure  $^{238}\text{U}$  was obtained by us [11,40] by using fission track etch-cum gamma ray spectrometric technique. In this method the photo peak activity ( $A_x$ ) of any fission product (X) is related to the absolute fission yield ( $Y_x$ ) as

$$A_x = F I \gamma \varepsilon Y_x (1 - e^{-\lambda t}) e^{-\lambda T} \quad (5)$$

where  $t$  and  $T$  are the irradiation and cooling time, respectively. 'a' is the gamma ray abundance or branching intensity and  $\varepsilon$  the efficiency of the gamma ray in the detector system used.  $F$  is the total number of fission, given as

$$F = n \sigma \Phi t = (W \cdot T_d) / (K_{wet} \cdot C) \quad (6)$$

Where,  $n$  is the number of target atoms,  $\sigma$  the fission cross-section ( $\text{cm}^2$ ),  $\Phi$  the neutron flux ( $\text{cm}^{-2} \text{s}^{-1}$ ) and  $t$  irradiation time (s).  $W$  is the weight of target material (gm),  $K_{wet}$  is the efficiency factor for track registration in solution (cm) and  $C$ , the concentration of the dilute solution of the target material ( $\text{gm cm}^{-3}$ ) used for track registration.

From Eq. (5) and (6), the absolute fission product yield ( $Y_x$ ) is given as

Naik, H  
Kim, GN  
Suryanarayana, SV  
Kim, KS  
Lee, MW  
Sanjeev, G  
Nimje, VT  
Mittal, KC  
Ganesan, S  
Goswami, A

---

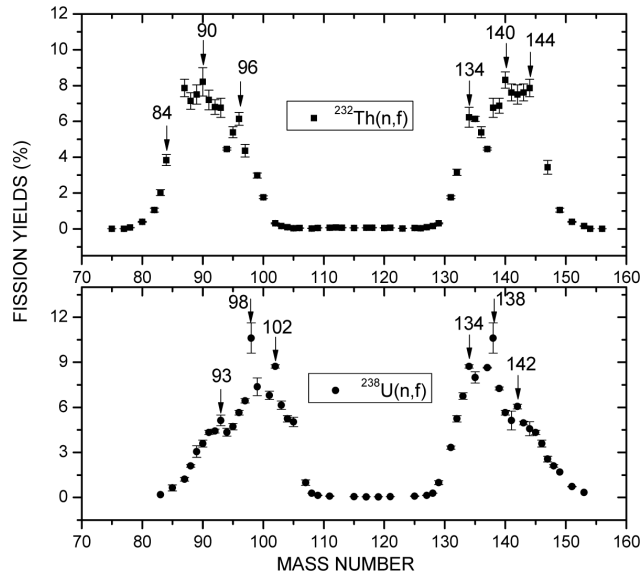


**Figure 1:** Yields of fission products as a function of mass number in the reactor neutron induced fission of  $^{232}\text{Th}$  and  $^{238}\text{U}$ .

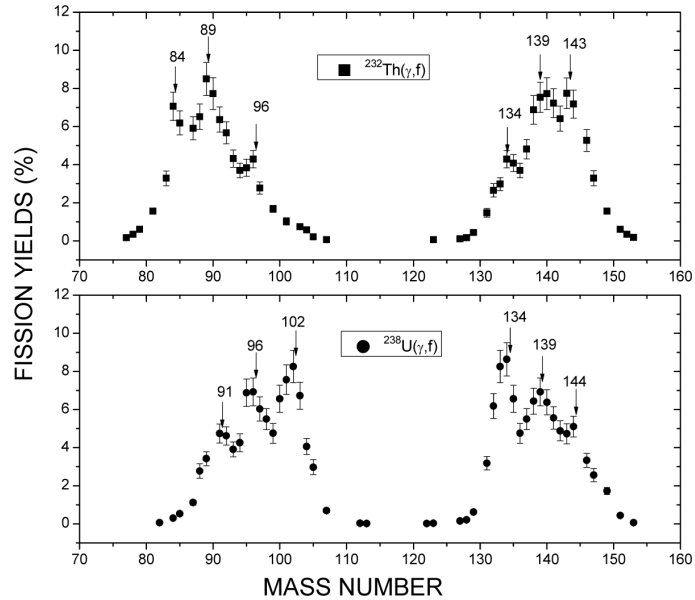


**Figure 2:** Yields of fission products as a function of mass number in the 8 MeV bremsstrahlung induced fission of  $^{232}\text{Th}$  and  $^{238}\text{U}$ .

$$Y_x = \frac{A_x}{I_{\gamma} \epsilon Y_X (1 - e^{-\lambda t}) e^{-\lambda T}} \frac{C \cdot K_{\text{wet}}}{W \cdot Td} \quad (7)$$

Studies on  
Neutron, Photon  
(Bremsstrahlung)  
and Proton  
Induced Fission of  
Actinides and  
Pre-Actinides

---

In the case of proton [10] and bremsstrahlung [8, 10, 12-19] induced fission of  $^{nat}\text{Pb}$ ,  $^{209}\text{Bi}$ ,  $^{232}\text{Th}$  and  $^{238}\text{U}$ , the relative cumulative yield ( $Y_x$ ) was obtained from the photo-peak activity ( $A_x$ ) of the fission product (X) using the equation (5). However, the individual yields of the fission products were first obtained with respect to a fission rate monitor. In the case of neutron and bremsstrahlung induced fission of  $^{232}\text{Th}$  and  $^{238}\text{U}$ , the fission product  $^{135}\text{I}$  was used as fission rate monitor. On the other hand in the bremsstrahlung induced fission of  $^{nat}\text{Pb}$  and  $^{209}\text{Bi}$ , the fission product  $^{103}\text{Ru}$  was used as the fission rate monitor. Then appropriate charge distribution correction [9-10, 13, 17-19, 35] was done to obtain the relative mass yields for different mass chains. Finally the mass chain yields were normalised to 200 % to obtain the absolute yields of the fission products. In all the above calculations, the nuclear spectroscopic data such as half-life ( $T_{1/2}$ ) and branching intensity ( $I_{\gamma}$ ) were taken from refs. [5, 24].

#### 4. RESULTS AND DISCUSSION

The yields of fission products in the reactor neutron induced fission of actinides such as  $^{232}\text{Th}$  (n, f) [39] and  $^{238}\text{U}$  (n, f) [11] determined in the Radiochemistry Division, BARC using APSARA reactor are presented in the Fig. 1. Similarly, the mass chain yields of various fission products in the 8 MeV bremsstrahlung induced fission of  $^{232}\text{Th}$  and  $^{238}\text{U}$  from the work carried out at microtron centre, Mangalore [18] are plotted in the Fig. 2. This was done because the excitation energy of the 8 MeV bremsstrahlung and reactor neutron induced fission of  $^{232}\text{Th}$  and  $^{238}\text{U}$  have the comparable excitation energy. The excitation energies for the 8 MeV Bremsstrahlung induced fission of  $^{232}\text{Th}$  and  $^{238}\text{U}$  are 6.52 and 6.53 MeV, respectively. Similarly, the excitation energies for the reactor neutron induced fission of  $^{232}\text{Th}$  and  $^{238}\text{U}$  are 6.51 and 6.25 MeV, respectively. This is because the reactor neutron has average neutron energy of 1.9 MeV [11, 39-40].

It can be seen from Figs. 1 and 2 that in the reactor (i.e. 1.9 MeV) neutron and 8 MeV Bremsstrahlung induced fission of  $^{232}\text{Th}$  and  $^{238}\text{U}$ , the yields of fission products around mass numbers 133-134, 138-140 and 143-144 and their complementary products are higher than the other fission products. The higher yields of the fission products around the mass numbers 133-134 and 143-144 and their complementary products can be explained from the point of view of the standard I and standard II asymmetric fission modes mentioned

Naik, H  
Kim, GN  
Suryanarayana, SV  
Kim, KS  
Lee, MW  
Sanjeev, G  
Nimje, VT  
Mittal, KC  
Ganesan, S  
Goswami, A

---

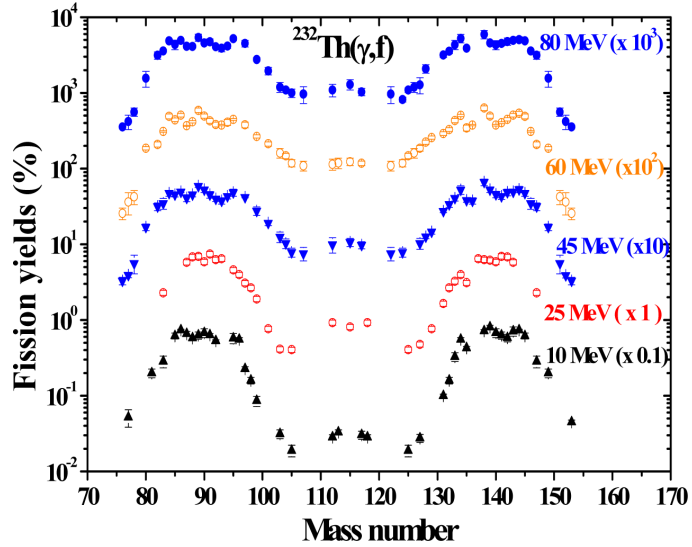


**Figure 3:** Yields of fission products as a function of mass number in the 10-80 MeV bremsstrahlung induced fission of  $^{232}\text{Th}$ .

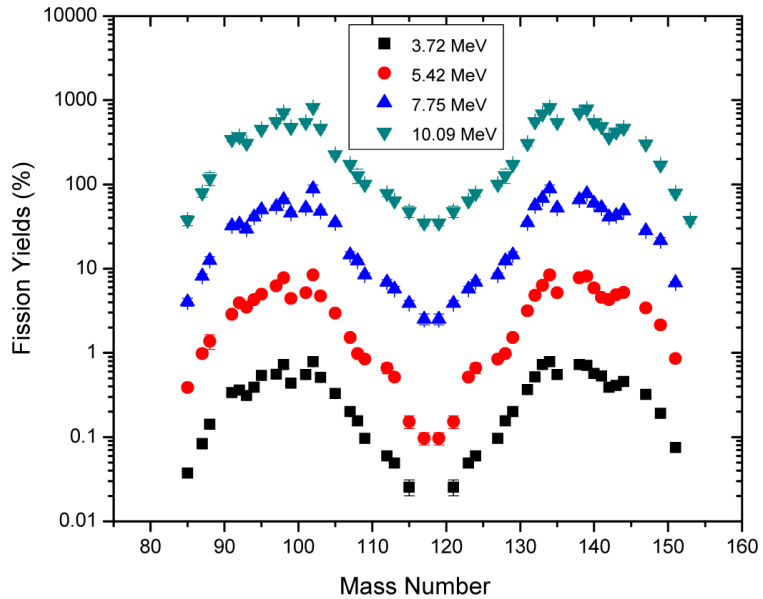


**Figure 4:** Yields of fission products as a function of mass number in the 3.7-10.1 MeV quasi-mono-energetic neutron induced fission of  $^{238}\text{U}$ .

by Brossa *et al.* [41], which arise due to shell effects [2]. Based on standard I asymmetry, the fissioning system is characterized by spherical heavy fragment mass with  $A=133-134$  and  $Z_p=52$  due to the approach of spherical shell closure at  $N=82$  and a deformed complementary light mass number. Thus the higher yields of the fission products such as  $^{133}\text{I}$  and  $^{134}\text{Te}-^{134}\text{I}$  is due to the presence of spherical neutron shell at  $N=82$ . The neutron number of 82 is based on the assumption of one neutron emission for  $A=133-134$  with most probable charge ( $Z_p$ ) of 52. Similarly, based on standard II asymmetry, the fissioning system is characterized by a deformed heavy fragment mass with  $A=143-144$  and  $Z_p=54$  due to the approach of deformed shell closure at  $N=88$  and slightly deformed light mass. The neutron number of 88 is based on the assumption of 2 neutron emission for  $A=143-144$  with most probable charge ( $Z_p$ ) of 56. Thus, the higher yields of fission products  $^{133}\text{I}$  and  $^{134}\text{Te}-^{134}\text{I}$  and their complementary products as well as for  $^{143,144}\text{Ce}$  and their complementary products are due to the presence of spherical shell closure at  $N=82$  and deformed shell closure at  $N=88$ , respectively. On the other hand, the higher yields of fission products  $^{138}\text{Xe}$ - $^{138}\text{Cs}$ ,  $^{139-140}\text{Ba}$  and their complementary products are not possible to explain based on only standard I and standard II asymmetric fission modes [41] unless even-odd effect is considered. As can be seen, for the mass numbers 133-134, 138-140 and 143-144, the higher yields of the heavy and light complementary mass fission products are in the interval of five mass and two charge units. The most probable charge corresponding to the masses of 133-134, 138-140 and 143-144 are even  $Z$  at 52, 54 and 56, which results the  $A/Z$  values of 2.5. Thus the difference of two even charges causes the higher mass chain yields in the interval of five mass units. This indicates the role of even-odd effect besides shell effect. However, the effect of nuclear structure decreases with increase of excitation energy.

The role of excitation energy on the fine structure can be examined from the mass yield distribution in the higher energy photon (bremsstrahlung), neutron and proton induced fission of  $^{232}\text{Th}$  and  $^{238}\text{U}$  [9-10, 13, 17-19, 35]. As an example, the mass yield distribution in the bremsstrahlung induced fission of  $^{232}\text{Th}$  determined using 10 MeV electron linac of EBC, Kharghar, Navi-Mumbai, India [35] and 100 MeV electron linac of PAL, Pohang, South Korea [9-10, 13, 17-19, 35] are shown in Fig. 3. Similarly, the mass yield distribution in the higher energy neutron induced fission of  $^{238}\text{U}$  determined at BARC-TIFR facility using  $^7\text{Li}(p, n)$  reaction are shown in Fig. 4. On the other hand, the mass yield distribution in the proton induced fission of  $^{232}\text{Th}$  for 20 MeV at BARC-TIFR Pelletron facility, Mumbai, India and for 32 and 45 MeV at KIRAMS, Seoul, South Korea is presented in Fig. 5. From the Figs. 3-5, decrease trend of fine structure with increase of excitation energy can be very well observed.

Naik, H  
 Kim, GN  
 Suryanarayana, SV  
 Kim, KS  
 Lee, MW  
 Sanjeev, G  
 Nimje, VT  
 Mittal, KC  
 Ganesan, S  
 Goswami, A

---

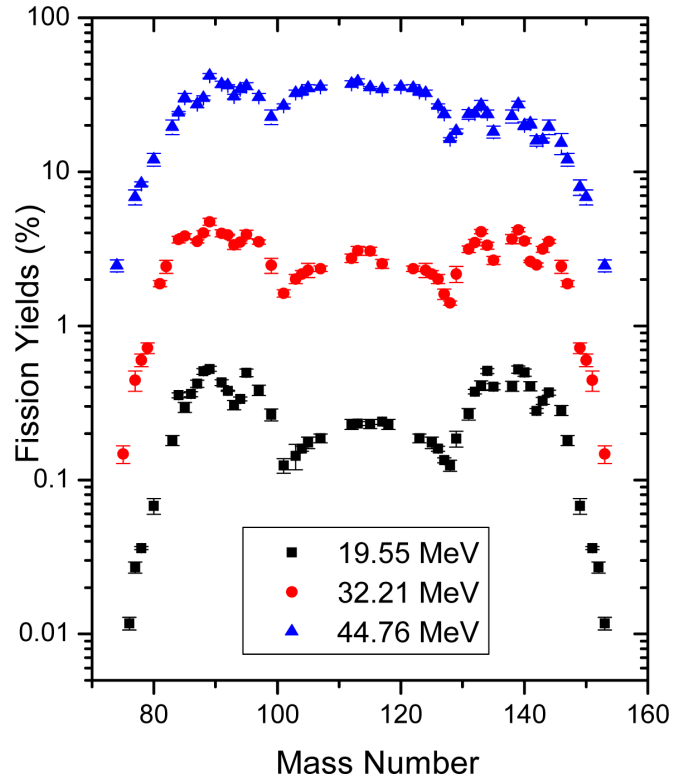


**Figure 5:** Yields of fission products as a function of mass number in the 20-45 MeV proton induced fission of  $^{232}\text{Th}$ .

Further from Fig. 3-5, it can be seen that the yields of symmetric fission products in the photon (bremsstrahlung), neutron and proton induced fission of  $^{232}\text{Th}$  and  $^{238}\text{U}$  increase with increase of projectile energy. On the other hand, the yield of asymmetric products decreases with excitation energy. This is to conserve the mass yield distribution of 200 percent. In view of this the yield of asymmetric fission products in the photon (bremsstrahlung), neutron and proton induced fission of  $^{232}\text{Th}$  and  $^{238}\text{U}$  are plotted in Fig. 6 as a function of compound nucleus excitation energy. On the other hand, the yield of symmetric products and thus the peak-to-valley ratio (P/V) i.e. yield of the asymmetric to symmetric fission products are plotted in the Fig. 7 as a function of compound nucleus excitation. The excitation energy ( $E^*$ ) of the compound nucleus ( $A_c$ ) corresponding to the neutron ( $E_n$ ) and proton ( $E_p$ ) are calculated using the following relation.

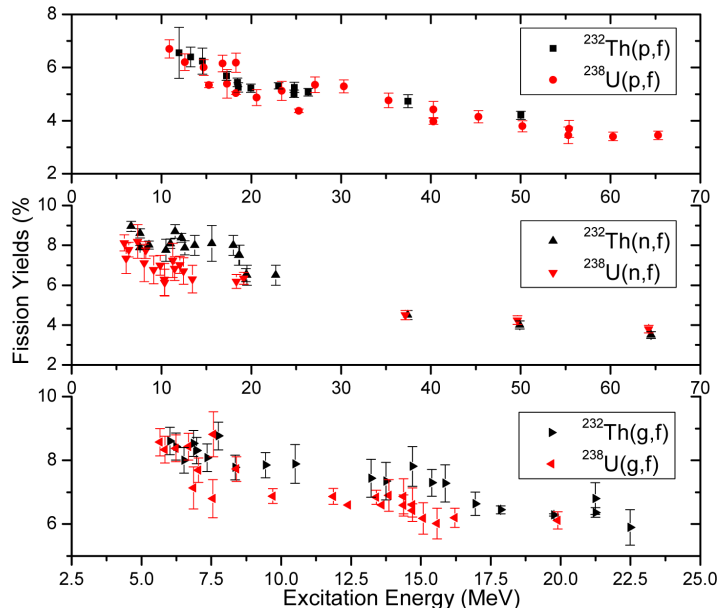


**Figure 6:** Fission yields of asymmetric product as a function of excitation energy.

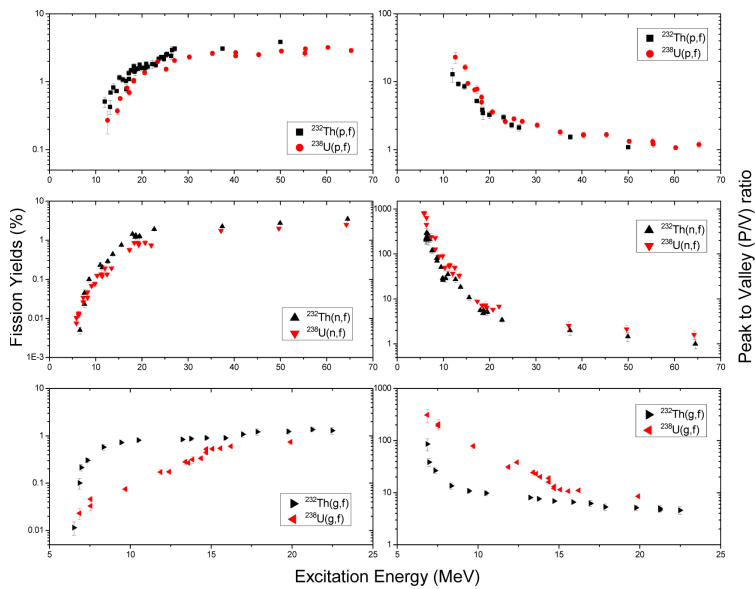


**Figure 7:** Fission yields of symmetric product and P/V ratio as a function of excitation energy.

Naik, H  
 Kim, GN  
 Suryanarayana, SV  
 Kim, KS  
 Lee, MW  
 Sanjeev, G  
 Nimje, VT  
 Mittal, KC  
 Ganesan, S  
 Goswami, A

---

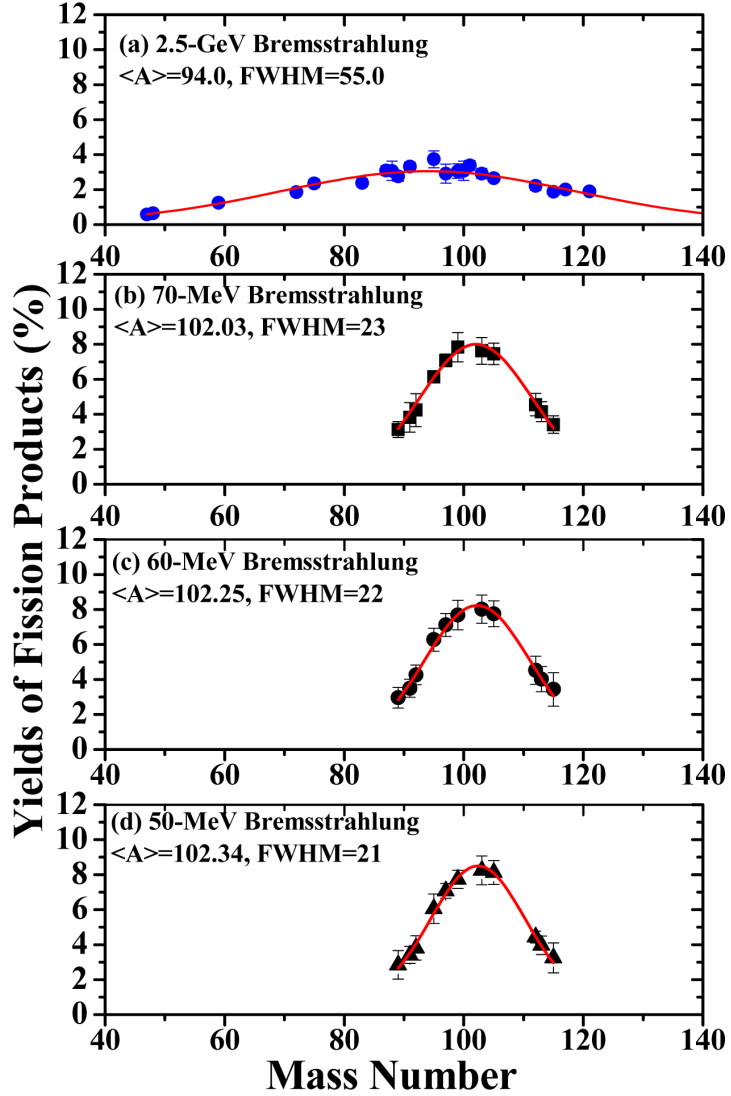


**Figure 8:** Yield of fission products in the bremsstrahlung induced fission of  $^{nat}\text{Pb}$ .

$$E_n^* = [(\Delta m^{232}\text{Th} (^{238}\text{U}) + \Delta m (n)) - \Delta m^{233}\text{Th} (^{239}\text{U})] + E_n \quad (8)$$

$$E_p^* = [(\Delta m^{232}\text{Th} (^{238}\text{U}) + \Delta m (^1\text{H})) - \Delta m^{233}\text{Pa} (^{239}\text{Np})] + E_p \quad (9)$$

The  $\Delta m$  value of  $^1\text{H}$ ,  $^{232,233}\text{Th}$ ,  $^{238,239}\text{U}$ ,  $^{233}\text{Pa}$  and  $^{239}\text{Np}$  were taken from the nuclear wallet cards [26]. In the case of photon induced fission of  $^{232}\text{Th}$  and

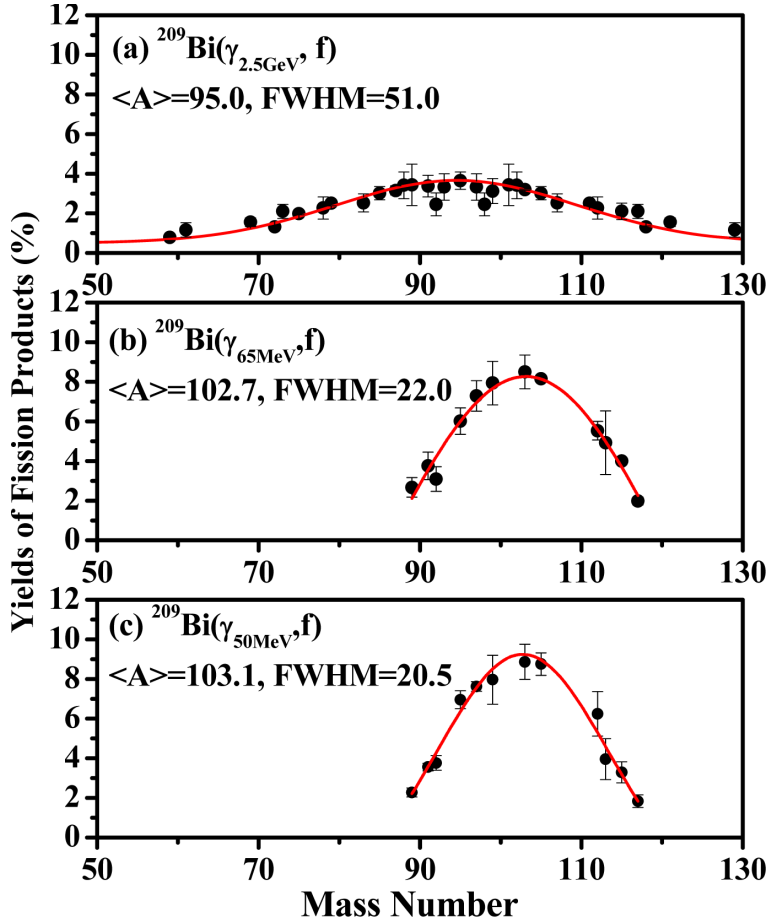


**Figure 9:** Yield of fission products in the bremsstrahlung induced fission of  $^{209}\text{Bi}$ .

$^{238}\text{U}$ , the excitation energy ( $E^*(E_e)$ ) of the compound nucleus corresponding to the end-point bremsstrahlung energy ( $E_e$ ) was calculated as [20]

$$\langle E^*(E_e) \rangle = \frac{\int_0^{E_e} E \cdot N(E_e, E_\gamma) \cdot \sigma_F(E_\gamma) dE_\gamma}{\int_0^{E_e} N(E_e, E_\gamma) \cdot \sigma_F(E_\gamma) dE_\gamma}, \quad (10)$$

where  $N(E_e, E_\gamma)$  is the number of photons with an energy  $E_\gamma$  produced from the incident electron energy  $E_e$  and  $\sigma_F(E_\gamma)$  is the fission cross-section as a function of the photon energy ( $E_\gamma$ ).

Naik, H  
 Kim, GN  
 Suryanarayana, SV  
 Kim, KS  
 Lee, MW  
 Sanjeev, G  
 Nimje, VT  
 Mittal, KC  
 Ganesan, S  
 Goswami, A

---

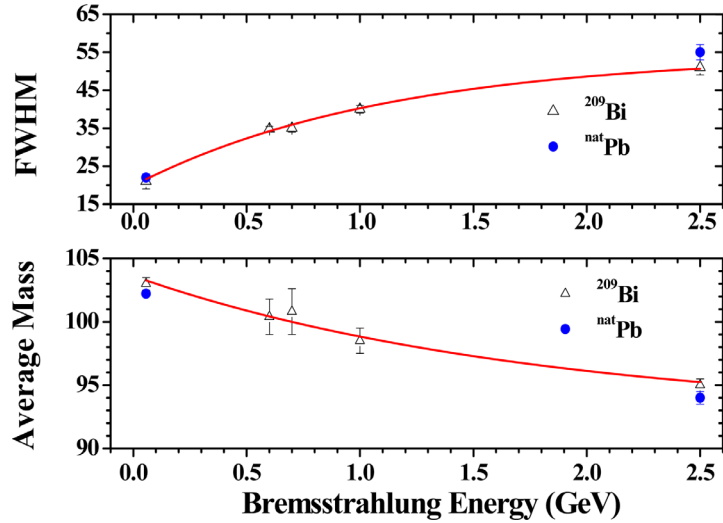


**Figure 10:** Average mass and FWHM of mass yield distribution in the bremsstrahlung induced fission of  $^{nat}\text{Pb}$  and  $^{209}\text{Bi}$ .

The bremsstrahlung spectrum  $N(E_e, E_\gamma)$  corresponding to an incident electron energy ( $E_e$ ) was calculated using the EGS4 computer code [43], as is usually done [8, 10, 12-17, 19]. Thus the photo-fission cross-section of  $^{232}\text{Th}$  and  $^{238}\text{U}$  as a function of photon energy was calculated using the TALYS code version 1.2 [1].

It can be seen from Fig. 6 that in the photon (bremsstrahlung), neutron and proton induced fission of  $^{232}\text{Th}$  and  $^{238}\text{U}$ , the yields of asymmetric products for  $A=133-134$ ,  $139-140$  and  $143-144$  decrease slowly with increase of excitation energy. On the other hand, it can be seen from Fig. 7 that the yields of symmetric products increase and thus the P/V ratio decrease with excitation energy. These observations indicate the role of excitation energy.

Besides these above observations, it can be seen from Figs. 3-5 that the photon, neutron and proton induced fission of  $^{232}\text{Th}$  and  $^{238}\text{U}$ , the mass yield distribution are asymmetric one with triple and double humped, respectively. This is because the different type of outer potential fission barrier for  $^{232}\text{Th}$  compared to  $^{238}\text{U}$  [36]. On the other hand, potential barrier of pre-actinides fission follows the liquid drop fission barrier. Thus the mass yield distribution in the photon (bremsstrahlung), neutron and proton induced fission of pre-actinides such as  $^{nat}\text{Pb}$  and  $^{209}\text{Bi}$  are symmetric with single humped [8, 12, 14-16]. As an example, the mass yield distribution in the 50-70 MeV and 2.5 MeV bremsstrahlung induced fission of  $^{nat}\text{Pb}$  and  $^{209}\text{Bi}$  determined using electron

linac of PAL, South Korea are shown in Fig. 8 and Fig. 9, respectively. It can be seen from Fig. 8 and Fig. 9 that the mass yield distribution becomes wider and the average mass shift to lower mass with increase of end-point bremsstrahlung energies, which can be seen from Fig. 10. This indicates the role of excitation energy.

## CONCLUSIONS

- (i) In the photon (bremsstrahlung), neutron and proton induced fission of actinides such as  $^{232}\text{Th}$  and  $^{238}\text{U}$ , the yields of fission products around  $A=133-134$ ,  $138-140$ ,  $143-144$  and complementary products are higher than the other fission products, which is due to the role of nuclear structure such as effect of shell closure proximity and even-odd effect.
- (ii) In actinide fission, the yields of symmetric products increase with excitation energy. On the other hand the yield of asymmetric products and P/V ratio decrease with excitation energy, which indicates the role of excitation energy.
- (iii) The mass yield distribution in the photon (bremsstrahlung), neutron and proton induced fission of  $^{232}\text{Th}$  and  $^{238}\text{U}$  are asymmetric with triple and double humped, whereas it is symmetric with single humped in  $^{\text{nat}}\text{Pb}$  and  $^{209}\text{Bi}$ . This due to the different types of potential fission barrier for actinides and pre-actinides.

## ACKNOWLEDGEMENT

The authors are thankful to the staff of reactor APSARA at BARC, microtron, at Mangalore University, Karnataka, electron linac at EBC, Kharghar, Navi-Mumbai, at PAL, Pohang, South Korea and medical cyclotron (KIRAMS) at Seoul, South Korea for their excellent co-operation and help during experiment.

## REFERENCES

- [1] A. J. Koning, S. Hilaire, and M.C. Duijvestijn, Proceedings of the International Conference on Nuclear Data for Science and Technology-ND 2004, AIP Vol. **769**, Sept. 26- Oct. 1 (2004), Santa Fe, USA (2005) P. 1154.
- [2] B.D. Wilkins, E.P. Steinberg, R.R. Chasman, Phys. Rev. C **14**, 1832 (1976).
- [3] B.F. Rider, Compilation of fission products yields, NEDO, 12154 3c ENDF-327, Valescicecitos Nuclear Centre, 1981.
- [4] C. Wagemans, The Nuclear Fission Process (CRC, London, 1990).
- [5] E. Browne and R.B. Firestone, Table of Radioactive Isotopes, ed. V.S. Shirley (1986); R. B. Firestone and L. P. Ekstrom, Table of Radioactive Isotopes, (2004).

- 
- Naik, H  
Kim, GN  
Suryanarayana, SV  
Kim, KS  
Lee, MW  
Sanjeev, G  
Nimje, VT  
Mittal, KC  
Ganesan, S  
Goswami, A
- 
- [6] E. Fermi, E. Amaldi, O. D'Agostino, F. Rasetti and E. Segre, Proc. Roy. Soc. (London) **146**, 483 (1934).
- [7] E. Fermi, Nature **133**, 898 (1934).
- [8] H. Naik, G. N. Kim, A. Goswami, S. Singh, V. K. Manchanda, D. Raj, S. Ganesan, Y. D. Oh, H.-S. Lee, K. S. Kim, M.-W. Lee, M.-H. Cho, I. S. Ko, and W. Namkung. J. Radioanal. Nucl. Chem. **283**, 439 (2010).
- [9] H. Naik, A. Goswami, G. N. Kim, K. Kim and S. V. Suryanarayana. Eur. Phys. J. A **49** (133), 1-16 (2013).
- [10] H. Naik, A. Goswami, G. N. Kim, M. W. Lee, K.S. Kim, S. V. Suryanarayana, E. A. Kim and M.-H. Cho. Phys. Rev. C. **86**, 054607 (2012).
- [11] H. Naik, A.G.C. Nair, P.C. Kalsi, A.K. Pandey, R.J. Singh, A. Ramaswami, R. H. Iyer, Radiochim.Acta **75**, 69 (1996).
- [12] H. Naik, A.V.R. Reddy, S. Ganesan, D. Raj, K. Kim, G. Kim, Y.D. Oh, D.K. Pham, M.-H. Cho, I.S. Ko, W. Namkung, J. Kor. Phys. Soc. **52**, 934 (2008).
- [13] H. Naik, B.S. Shivashankar, H.G. Raj Prakash, Devesh Raj, Ganesh Sanjeev, N. Karunakara, H.M. Somashekarappa, S. Ganesan and A. Goswami. J. Radioanal. Nucl. Chem. **299**, 127 (2014).
- [14] H. Naik, S. Singh, A. Goswami, V. K. Manchanda, S.V. Suryanarayana, D. Raj, S. Ganesan, Md. S. Rahman, K. S. Kim, M. W. Lee, G. N. Kim, M.-H. Cho, I. S. Ko and W. Namkung, Eur. Phys. J. A **47**, 37 (2011).
- [15] H. Naik, S. Singh, A.V.R. Reddy, V.K. Manchanda, S. Ganesan, D. Raj, Md. Shakilur Rahman, K.S. Kim, M.W. Lee, G. Kim, Y.D. Oh, H.-S. Lee, M.-H. Cho, S. Ko, and W. Namkung, Eur. Phys. J. A **41**, 323 (2009).
- [16] H. Naik, Sarbjit Singh, A. V. R. Reddy, V. K. Manchanda, G. Kim, K. S. Kim, M.W. Lee, S. Ganesan, D. Raj, H. S. Lee, Y.D. Oh, M. H. Cho, I. S. Ko, W. Namkung, Nucl. Instruments Methods in Phys. Research B **267**, 1891 (2009).
- [17] H. Naik, T.N. Nathaniel, A.Goswami, G.N. Kim, M.W. Lee, S.V. Suryanarayana S. Ganesan, E.A. Kim, M.-H. Cho, K.L. Ramakumar, Phys. Rev. C **85**, 024623-1 (2012).
- [18] H. Naik, V. K. Mulik, P. M. Prajapati, B. S. Shivasankar, S. V. Suryanarayana K. C. Jagadeesan, S. V. Thakare, S. C. Sharma and A. Goswami. Nucl. Phys. A **913**, 185 (2013).
- [19] H. Naik, V.T. Nimje, D.Raj, S.V. Suryanarayana, A. Goswami, Sarbjit Singh, S. N. Acharya, K.C. Mittal, S. Ganesan, P. Chandrachoodan, V.K. Manchanda, V. Venugopal, S. Banarjee, Nucl. Phys. A **853** (2011) 1. <http://dx.doi.org/10.1016/j.nuclphysa.2011.01.009>
- [20] H. Thierens, D. De Frenne, E. Jacobs, A. De Clercq, P. D'hondt, and A.J. Deruytter, Phys. Rev. C **14**, 1058 (1976).
- [21] I. Cuire and P. Savitch, J. de. Phys. **7** (8), 385 (1937).
- [22] I. Curie and F. Joliot, Comptes Rendus **198**, 254 (1934).
- [23] IAEA-EXFOR Database, at <http://www-nds.iaea.org/exfor>.
- [24] J. Blachot and Ch. Fiche, Table of Radioactive Isotopes and their main decay characteristics, Ann. de Phys. **6**, 3 (1981).
- [25] J. Chadwick, Proc. Roy. Soc. (London) **136**, 692 (1932).
- [26] J. K. Tuli, Nuclear Wallet Cards, National Nuclear Data Center, Brookhaven National Laboratory, Upton, New York 11973-5000, USA (2011) [<http://www.nndc.bnl.gov>].
-

- 
- [27] J.R. England, B.F. Rider, Evaluation and compilation of fission products yields, ENDF/BVI, 1989, 1992.
- [28] L. Meitner, and O.R. Frisch, Nature **143**, 239 (1939).
- [29] M. James, R. Mills, Neutron fission products yields, UKFY2, 1991; JEF-2.2, 1993.
- [30] N. Bohr and J.A. Wheeler, Phys. Rev. **56**, 426 (1939).
- [31] N. Bohr, Phys. Rev. **55**, 418 (1939).
- [32] O. Hahn and F. Strassmann, Naturwiss **26**, 756 (1937).
- [33] O.R. Frisch, Nature **143**, 276 (1939).
- [34] P. Fong, Phys. Rev. **102**, 434 (1956).
- [35] P. M. Prajapati, H. Naik, S. Mukherjee, S. V. Suryanarayana, B.S. Shivashankar, R. Crasta, V. K. Mulik, K. C. Jagadeesan, S. V. Thakre and A. Goswami, Nucl. Sci. Eng. **176**, 1 (2014).
- [36] P. Moller, Nucl. Phys.A **192**, 529 (1972).
- [37] P. Moller, S.G. Nilsson, A. Sobiczewski, Z. Szymanski, S. Wycech, Phys. Lett. B-30, **223** (1969).
- [38] R. Vandenbosch and J.R.Huizenga, Nuclear Fission (Academic, New York, 1973).
- [39] R.H. Iyer, C.K. Mathewes, N. Ravindran, K. Rengan, D.V. Singh, M.V. Ramaniah and H.D. Sharma, J. Inorg. Nucl. Chem. **25**, 465 (1965).
- [40] R.H. Iyer, H. Naik, A.K. Pandey, P.C. Kalsi, R.J. Singh, A. Ramaswami, A. G. C. Nair, Nucl. Sci. Eng. **135**, 227 (2000).
- [41] U. Brossa, S. Grossmann, A. Muller, Phys. Rep. **197**, 167 (1990).
- [42] V. M. strutinsky, JETP (USSR) 45, 1900 (1963); V. M. strutinsky, Sov. Phys. JETP **18**, 1900 (1963).
- [43] W. R. Nelson, H. Hirayama, and D.W.O Rogers, MAC report 265 (1985).

Studies on  
Neutron, Photon  
(Bremsstrahlung)  
and Proton  
Induced Fission of  
Actinides and  
Pre-Actinides

---